

## Characterization of the geothermal reservoir potential of the Permocarboniferous in the northern Upper Rhine Graben, Germany

Achim Aretz, Kristian Bär and Ingo Sass

Technische Universität Darmstadt, Institute of Applied Geosciences, Chair of Science and Technology,  
Schnittspahnstraße 9, D - 64287 Darmstadt

aretz@geo.tu-darmstadt.de

**Keywords:** northern Upper Rhine Graben, Saar-Nahe Basin, Permocarboniferous, Geothermics, Outcrop Analogue Studies

### ABSTRACT

The Permocarboniferous is the biggest hydrothermal reservoir in the northern Upper Rhine Graben and has so far been investigated in large scale studies only. To further assess the geothermal reservoir potential of the different lithostratigraphical units and facies types within this variscan intramontane basin, knowledge of their thermophysical and hydraulic properties is essential. Where the Cenozoic Upper Rhine Graben crosses the Permocarboniferous molasse basin, the top of the up to 2 km thick formation is located at a depth of 1 to 3 km and is overlain by Tertiary and Quaternary sediments. At this depth the reservoir temperatures exceed 150 °C, making it suitable for geothermal power generation. The Permocarboniferous deposits are subdivided in different subgroups and consist lithologically of several facies types including fine-, middle- and coarse-grained sandstones, arcic sandstones, siltstones, volcanics and subsidiary carbonates. Within the scope of this study, outcrop analogue studies west of the Graben in the Saar-Nahe Basin, and east of the Graben in the Sprenzlinger Horst, Wetterau and the Wetterau-Fulda Basin are conducted. Each lithostratigraphic formation and lithofacies type is sampled at various outcrops, so that a sufficient amount of samples of the different sedimentary rock types is available in order to evaluate their petrophysical, sedimentological and geochemical characteristics statistically. The petrophysical parameters measured include porosity, permeability, density, thermal conductivity, thermal diffusivity and uniaxial compressive strength. So far, the petrophysical properties of more than 80 locations have been determined, showing a clear correlation with the facies type. Among the stratigraphical units, Glan-Subgroup's and the Nahe-Subgroup's porosity averages to 16.4 % and 15.4 %, permeability to  $3.3 \cdot 10^{-15} \text{ m}^2$  and  $1.1 \cdot 10^{-16} \text{ m}^2$ , thermal conductivity to  $2.3 \text{ W/(m·K)}$  and  $2.0 \text{ W/(m·K)}$  and thermal diffusivity to  $1.4 \cdot 10^{-6} \text{ m}^2/\text{s}$  and  $1.2 \cdot 10^{-6} \text{ m}^2/\text{s}$  respectively. Additionally, the hydraulic conductivity of the reservoir was studied, using data of about 400

hydraulic tests conducted in 230 wells within the outcrop analogue area and were correlated to the stratigraphic units, the distance to the nearest fault and its orientation. Based on drilling and seismic data as well as geologic maps together with the compiled petrophysical and hydraulic data, it is intended to establish a 3D reservoir model of the Permocarboniferous in the northern Upper Rhine Graben and western Saar-Nahe Basin. Due to the importance of fault zones, lithostratigraphical units and facies types, detailed modeling will allow a better prediction of reservoir temperatures and production rates and will subsequently allow a better prognosis of the exploration risk.

### INTRODUCTION

The Permocarboniferous is the biggest hydrothermal reservoir in the northern Upper Rhine Graben and has been investigated in large scale studies (Arndt et al., 2011, Bär et al., 2011, Sass & Hoppe, 2011). Where the Cenozoic Upper Rhine Graben crosses the Permocarboniferous molasse basin the top of the up to two kilometers thick Permocarboniferous deposits

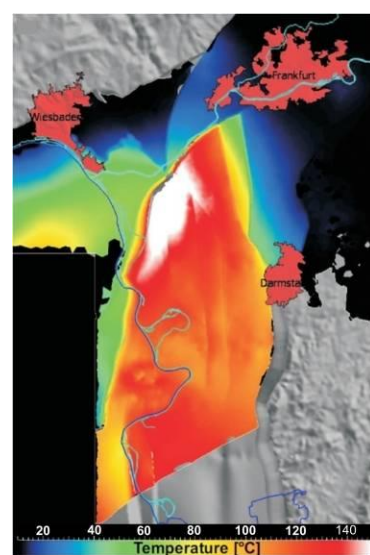


Figure 1: The mean reservoir temperature of the Permocarboniferous in the northern Upper Rhine Graben (Bär et al., 2011); grey = areas with no Permocarboniferous deposits

covering approximately a 1,000 km<sup>2</sup> large area is located at a depth of one to three kilometers and is overlain by Tertiary and Quaternary sediments (Müller, 1996). The reservoir temperatures being modeled in the research project “3D-Modellierung der geothermischen Tiefenpotenziale von Hessen” (Hessen 3D) by Sass & Hoppe (2011) exceed 150°C and make the reservoir suitable for geothermal power generation (Fig. 1). To further assess the geothermal potential of the different lithostratigraphical units and facies types within this Variscan, intramontane basin, knowledge of their thermophysical and hydraulic properties is essential. Since only five drillings intersect the Permocarboniferous in the northern Upper Rhine Graben outcrop analogue studies west and east of the graben have been conducted. Outcrop analogue studies are a well established method in the hydrocarbon industry (Jahn et al., 2008) that can be used optimally for the analysis of the relevant thermophysical and hydraulic geothermal reservoir parameters. Furthermore, pumping data sets available at state geological surveys (Hessisches Landesamt für Umwelt und Geologie (HLUG) and Landesamt für Bergbau und Geologie, Rheinland-Pfalz (LGB-RLP)) and oil companies (WEG e.V.) have been evaluated. The resulting data can be converted to the existing pressure and temperature conditions in the reservoir with the help of empirically determined equations that

have been applied in the hydrocarbon exploration for decades. A 3D reservoir model can visualize potential target horizons for deep geothermal realization and helps to make a prognosis of the exploration risk with a higher accuracy.

## GEOLOGY

The Permocarboniferous deposits are subdivided stratigraphically into the Glan-Subgroup, which is further subdivided from the base to the top into the Kusel-, Lebach- and Tholey- layers and into the overlying Nahe-Subgroup (Fig. 2). Lithologically these units consist of several facies types including fine, middle and coarse grained sandstones, arcose sandstones, siltstones, volcanics and carbonates (Schäfer, 2005). The deposition of the Permocarboniferous started in the Saar-Nahe Basin that is located west of the graben and extends over an area of 100 km x 40 km. During the deposition of the Kusel- and Lebach- layers, a progressing constriction of the Saar-Nahe Basin, an elevated relief of the provenance areas and the dominance of fluvial systems with a low sinuosity led to large deposits of coarse grained fluvial, deltaic and lacustrine sediments (Müller, 1996; Schäfer, 2005). During the deposition of the Tholey- layers a flattening of the Saar-Nahe Basin caused a reorganization of the

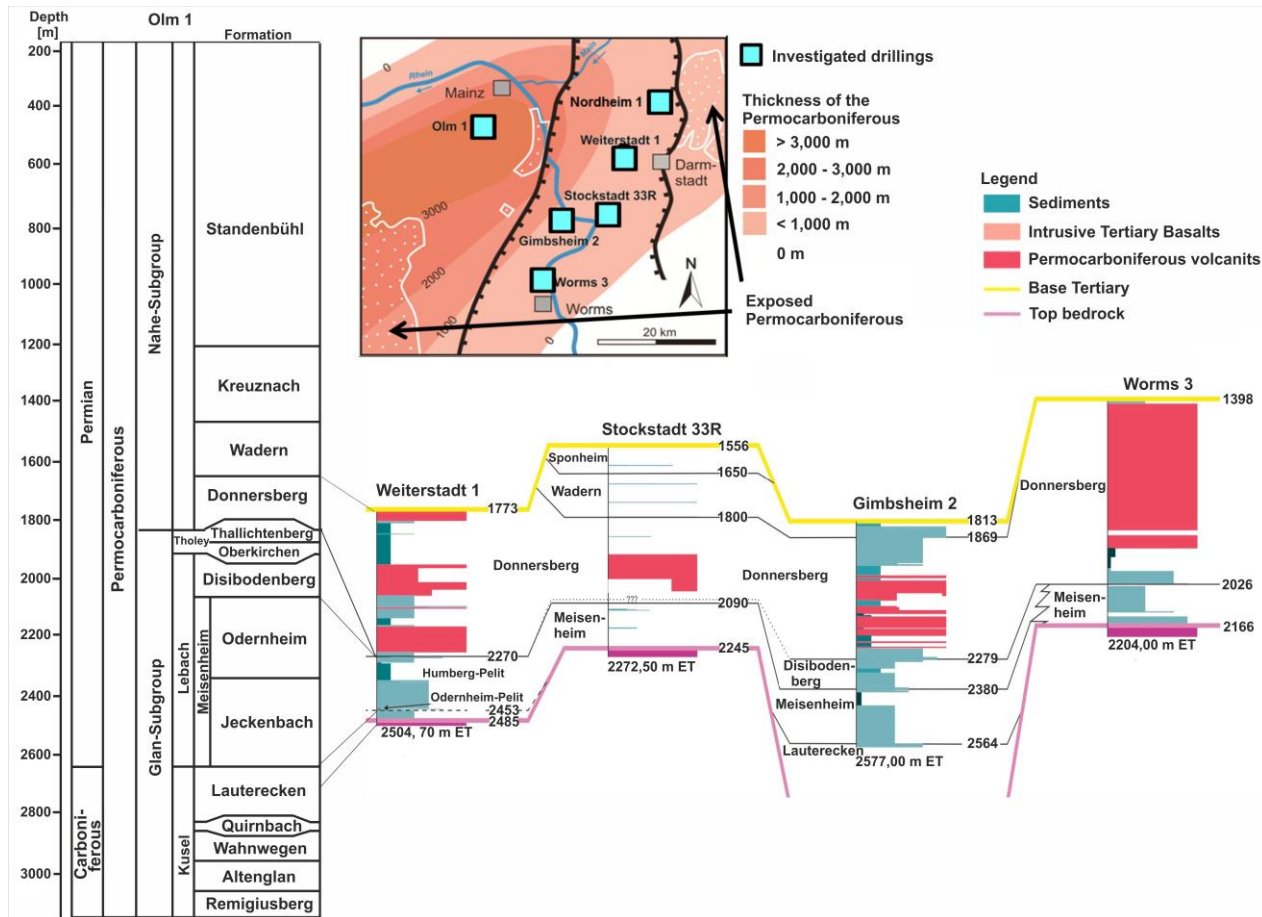


**Figure 2. The stratigraphy of the Permocarboniferous of different drillings and the Permocarboniferous thickness distribution in the northern Upper Rhine Graben und the Eastern Saar-Nahe Basin. after Becker et al. (2012) and Schäfer (2005)**

fluvial environments (Schäfer, 2005). The prevailing meandering systems crossed over a major variscan fault zone limiting the basin in the South and transported feldspar-rich, coarse grained sediments from the Vosges into the basin. This development is already associated with the imminent intrabasinal volcanism that marks the border between the Glan- and the Nahe-Subgroup (Stollhofen, 1998). The steep relief during the interphases of the volcanic eruptions supported a coarse-grained siliciclastic sediment transport from the surrounding areas (Stollhofen, 1994; 1998). The advancing subsidence at the Hunsrück Boundary Fault (HBF) bordering the basin in the Northwest caused on the one side conglomeratic- and breccia-rich alluvial fans that reach several kilometers into the basin and are summarized as the Wadern-Formation, and on the other side an advancing movement of the depocentre towards NE (Schäfer, 1989; Marell, 1989).

During this time the Sprendlinger Horst east of the graben was first affected by the sedimentation. With the begin of the post rift-phase the sedimentation was not controlled anymore by tectonic boundaries but by the thermal subsidence. So, the sedimentation stepped over the tectonic boundaries of the basin and even covered the Hunsrück on the other side of the HBF. The dominance of fluvial and eolian depositional environments in the basin led to the deposition of middle to coarse grained sediments forming the Kreuznach- and Sponheim- Formations. With the erosion of the volcanoes and a climate change towards arid conditions the basin geometry flattened again and Playa conditions became dominant. Red silt and fine

sand were deposited and finally formed the Nierstein-Formation (Schwarz et al., 2011). In the Oligocene a trans-European rift system was formed from the Mediterranean to the North Sea. The largest part of this system is the 300 km long and up to 40 km wide N-S trending Upper Rhine Graben (Walter & Dorn, 2007). Its subsidence that was the result of a WNW-ESE orientated crustal extension brought along the subsidence of the Permocarboniferous deposits and led to minimum total offset of 4.5 km at the main border faults of the graben.

## MATERIAL AND METHODS

In our study outcrop analogue studies have been conducted in the Saar-Nahe Basin west of and in the Sprendlinger Horst and in the Wetterau east of the northern Upper Rhine Graben (Fig. 3). So far, in the Saar-Nahe Basin approximately 70, in the Wetterau five and in the Sprendlinger Horst four outcrop locations have been sampled. Furthermore, drill cores in the Eastern Saar-Nahe Basin and the Sprendlinger Horst with lengths of 70 und 55 m respectively were investigated. Beyond that, 52 plugs from cores of the 5 drillings that intersected the Permocarboniferous in the northern Upper Rhine Graben in reservoir depths of 1,800 to 3,300 m were sampled.

The rock samples were cut in 20 to 30 mm high plugs being orientated parallel and orthogonal to bedding. At these plugs the porosity, permeability, thermal conductivity and thermal effusivity were measured. One thin section was prepared for petrographic analyses per sample. The porosity determination was accomplished by the measurement of the particle

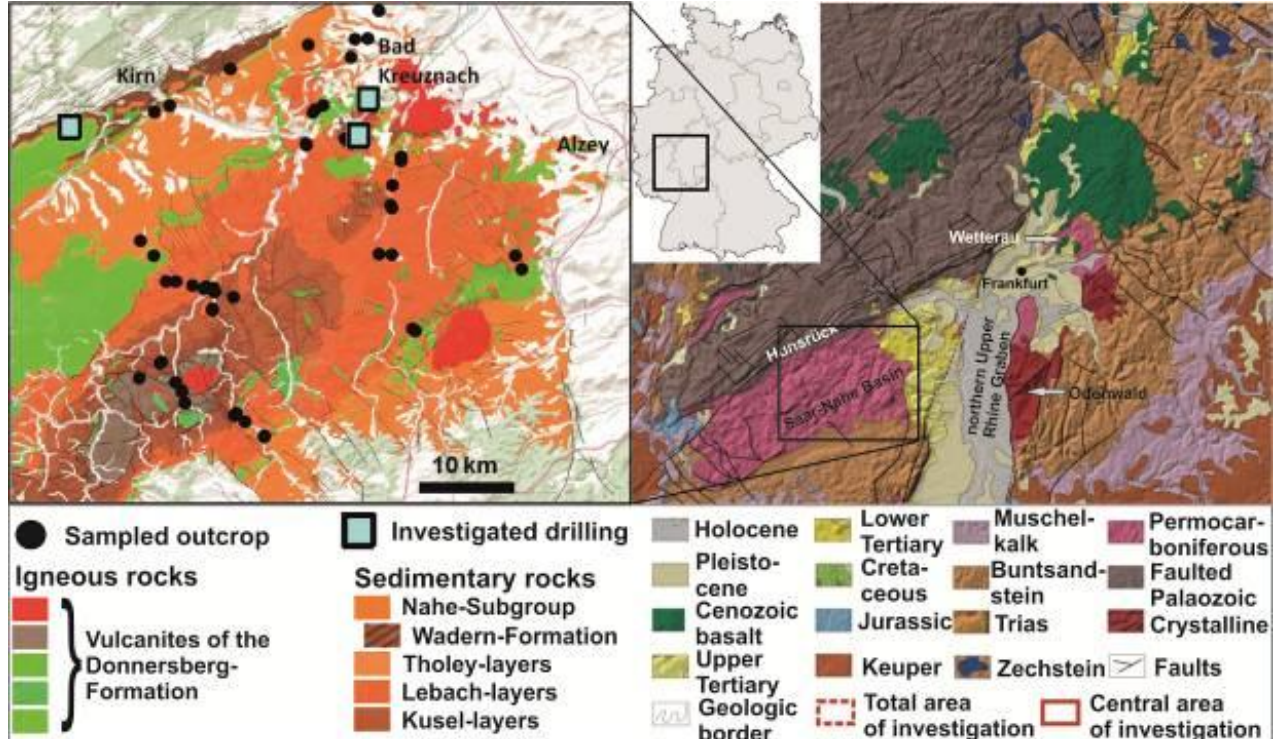


**Figure 3: An Overview over the outcrop analogue areas of the Permocarboniferous (right) and the position of the sampled outcrops and the investigated drillings in the Saar-Nahe Basin (left), after GÜK 200, LGB-RLP and Röhr (2006)**

density with a helium pycnometer (AccuPyc1330 from Micromeritics GmbH) and the bulk density with a powder pycnometer (Geopyc 1360 from Micromeritics GmbH). For the determination of the matrix permeability a pillar gas permeameter from Hornung & Aigner (2004) was used with which the apparent permeability is measured with the help of five single measurements at different pressure stages between 1 and 5 bar to calculate the intrinsic permeability (Klinkenberg, 1941). The thermal conductivity and diffusivity was measured with the optical thermal scanner (Fa. Lippmann and Rauen GbR: Lippmann & Rauen, 2005). The measurement is based on the optical scanning method with the use of infrared thermal sensors (Popov et al., 1983; 1999). Petrographic analyses to study the mineral composition, interconnectivity of the pore space, the kind of cement and the diagenesis characteristics completed the investigations. The latter play an important role to predict the influence of the diagenetic changes with depth on the different lithofacies types and its rock properties (Gaupp et al., 1993; Grötsch & Gaupp, 2011).

For the determination of the hydraulic conductivity Bär (2012) evaluated in the context of the research project Hessen 3D more than 400 pumping tests and other hydraulic data sets from 230 wells in the outcrop analogue area of the Permocarboniferous in the Saar-Nahe Basin, the Spindlinger Horst and the Wetterau with the help of the aquifer thickness, drawdown and the production rate (Sass & Hoppe, 2011). In the project presented here, approximately 100 of these data sets have been evaluated using AQTESOLV of HydroSolve Inc. which calculates the hydraulic conductivity on the basis of different type curves methods (Theis, 1935; Cooper & Jacob, 1946). A

correlation coefficient of 0.77 between the two methods shows that the hydraulic conductivities calculated by Bär (2012) can be considered as representative for the whole data set (Klaeske, 2012).

## RESULTS

The results were evaluated in terms of stratigraphy and lithofacies. In terms of the stratigraphic units the Tholey-layers show the highest porosities with 18.6 % and the highest permeabilities with  $2.3 \cdot 10^{-15} \text{ m}^2$  and the Lebach-layers the highest thermal conductivities

**Table 1: Overview over the geothermal outcrop parameters divided by stratigraphic units;  $\Phi$  = Porosity;  $K$  = Matrix permeability;  $\lambda$  = Thermal conductivity**

Stratigraphy	$\Phi$ [%]				$K$ [ $\text{m}^2$ ]				$\lambda$ [ $\text{W}/(\text{m} \cdot \text{K})$ ]			
	min	$\bar{x}$	max	n	min	$\bar{x}$	max	n	min	$\bar{x}$	max	n
Nahe-Subgroup	5.1	14.6	23.8	198	$1.1 \cdot 10^{-18}$	$3.6 \cdot 10^{-16}$	$1.3 \cdot 10^{-13}$	156	1.3	2.0	3.1	94
Glan-Subgroup	1.5	16.4	23.5	309	$3.7 \cdot 10^{-18}$	$1.1 \cdot 10^{-15}$	$7.8 \cdot 10^{-14}$	280	1.6	2.3	3.6	225
Tholey-layers	7.0	18.6	22.3	104	$1.7 \cdot 10^{-17}$	$2.3 \cdot 10^{-15}$	$7.8 \cdot 10^{-14}$	101	1.8	2.2	3.1	59
Lebach-layers	2.7	15.5	23.1	112	$5.1 \cdot 10^{-18}$	$3.8 \cdot 10^{-16}$	$5.3 \cdot 10^{-14}$	94	1.7	2.4	3.1	89
Kusel-layers	1.5	15.2	23.5	93	$3.7 \cdot 10^{-18}$	$6.8 \cdot 10^{-16}$	$1.4 \cdot 10^{-14}$	85	1.6	2.3	3.6	77

with 2.4  $\text{W}/(\text{m} \cdot \text{K})$  (Table 1). Reservoir samples exhibit with 6.9 % lower porosities and with  $2.0 \cdot 10^{-17} \text{ m}^2$  lower permeabilities than outcrop samples. Further investigations took place on a 70 m Permocarboniferous core drilled in the Eastern Saar-Nahe-Basin. The drilling profile consists mostly of fine to middle grained sandstone and intercalated thin mudstone layers. Sampling took place exemplarily at each core meter. The petrophysical parameters show a decrease with depth of e.g. the porosity from 24 to 12% of the permeability from  $1.0 \cdot 10^{-13}$  to  $2.0 \cdot 10^{-17} \text{ m}^2$  and an increase with depth of the thermal conductivity

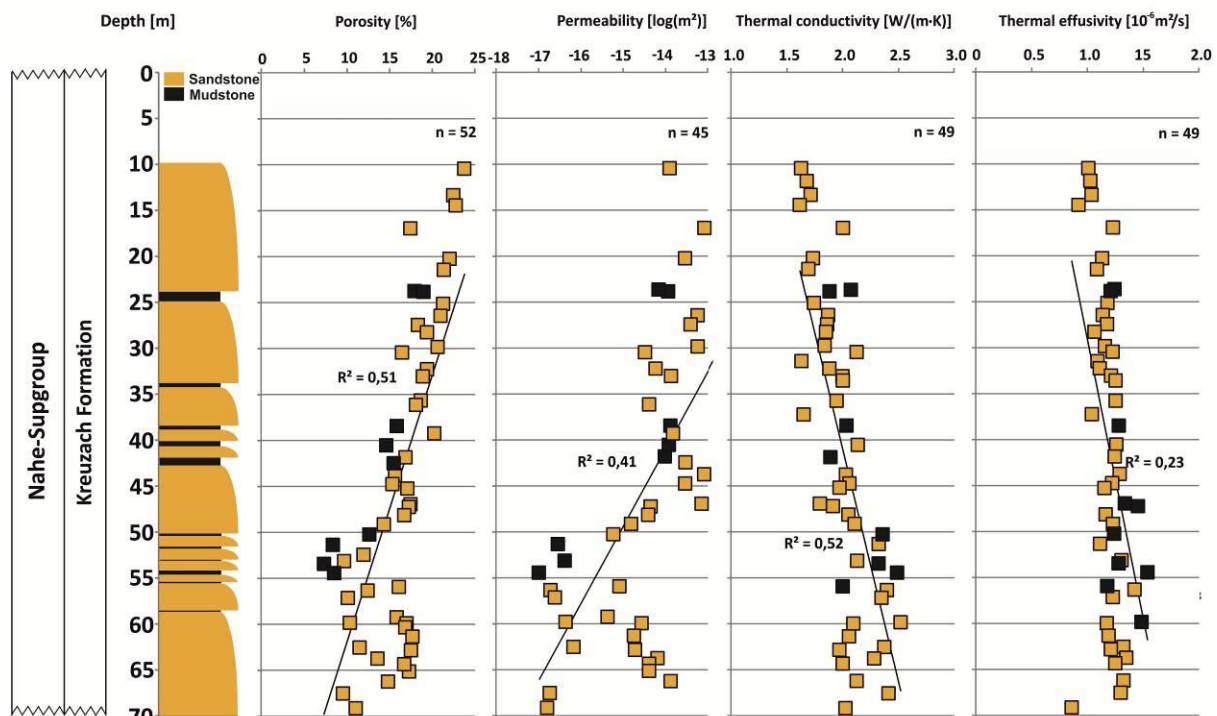


**Figure 4. Depth profiles of different geothermal parameters in the Kreuznach-Formation of the Eastern Saar-Nahe Basin near Bad Kreuznach**

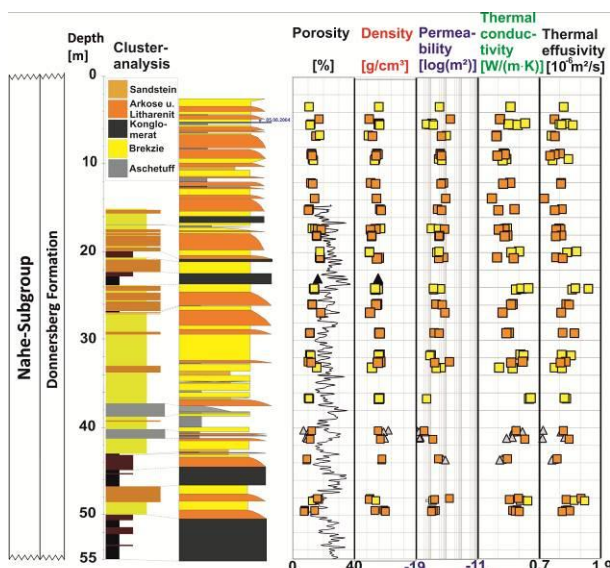


**Figure 5. Depth profiles of different geothermal parameters in the Donnersberg-Formation of the Sprendlinger Horst, Rüther (2011)**

from  $1.5$  to  $2.5$   $\text{W}/(\text{m}\cdot\text{K})$  and of the thermal diffusivity of  $0.6\cdot10^{-6}$  to  $1.6\cdot10^{-6}$   $\text{m}^2/\text{s}$  (Fig. 4). A second investigation of a drill core was done which was drilled east of the graben in the Sprendlinger Horst and consists in the upper 55 m of sandstones and tuffs of the Donnersberg-Formation of the Nahe-Subgroup (Fig. 5). The porosity ranges between 8 and 18 %, the permeability between  $3.0\cdot10^{-18}$  and  $1.0\cdot10^{-14}$   $\text{m}^2$ , the thermal conductivity between 1.7 and 2.8  $\text{W}/(\text{m}\cdot\text{K})$  and the thermal diffusivity between  $0.8\cdot10^{-6}$  and  $1.8\cdot10^{-6}$   $\text{m}^2/\text{s}$ . Petrographically the sandstones are classified using the nomenclature of Gazz (1966) and

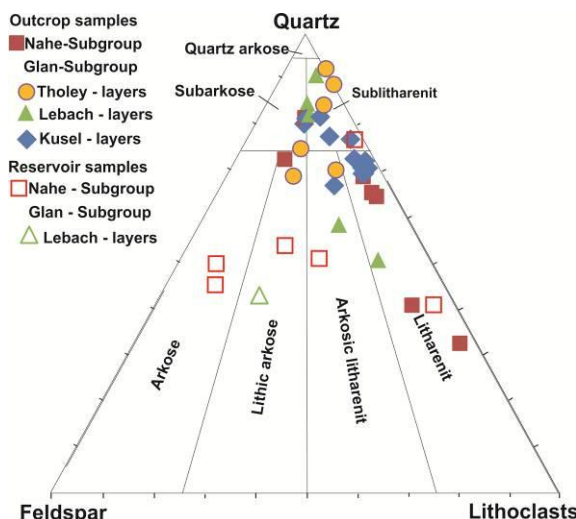


**Figure 6. The outcrop samples shower higher quartz contents than the reservoir samples, Gazz (1996), Dickinson (1970)**

Dickinson (1970) as subarkose ( $\text{Q}_{81} \text{F}_{10} \text{L}_9$ ), sublitharenit ( $\text{Q}_{84} \text{F}_4 \text{L}_{11}$ ) and litharenit ( $\text{Q}_{62} \text{F}_5 \text{L}_{32}$ ) (Fig. 6). Secondarily lithic arkose and arkosic litharenit occur. The reservoir samples consist of arkose, lithic arkose, arkosic litharenit and litharenit

mineral compositions and show quartz contents up to 20 % lower than the outcrop samples (Fig. 6). Considering the mineral composition of the outcrop samples the lithic arkose shows the highest porosities with 18% and the highest permeabilities with  $1.8\cdot10^{-14}$   $\text{m}^2$ , while the subarkose exhibits the highest thermal conductivities with  $2.4$   $\text{W}/(\text{m}\cdot\text{K})$ . Key for the prognosis of geothermal reservoir properties is the thermofacies concept of Sass and Götz (2012), according to which the permeability and the thermal conductivity being significantly responsible for the heat flow are dependent on the depositional facies. Fluvial facies types show a 15% higher quartz content and 15% lower lithoclast content than eolian and terrestrial facies types. Eolian facies types, indeed, are characterized by the highest porosities with 16.9 %, the highest permeabilities with  $2.5\cdot10^{-15}$   $\text{m}^2$ , the highest pore space filling amount of hematitic cement with 66 % and with 0.16 mm the highest grain size (Fig. 7). Playa facies types show the highest content of carbonatic cementation with 100% and fluviate facies types of illitic cementation with up to 49%.

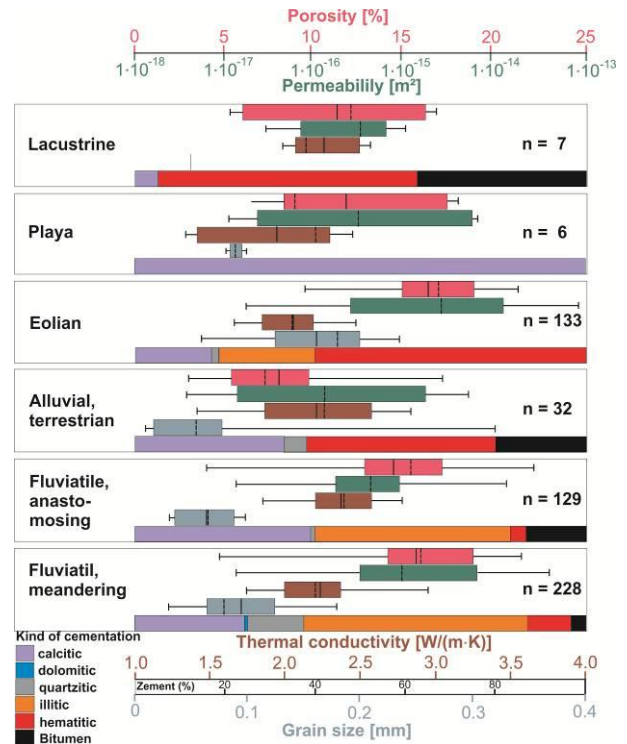


**Figure 7: Geothermal and petrographic parameters of different lithofacies types**

Considering the evaluation of the hydraulic conductivities of Bär (2012) and Klaeske (2012) the existing results were structured after stratigraphic units for the first time. The Glan- and Nahe-Subgroup with medium values of  $1.0\cdot10^{-6}$   $\text{m}/\text{s}$  each can be described as permeable after the DIN 18130 (Fig. 8). The Kreuznach-Formation in the Nahe-Subgroup shows with  $7.5\cdot10^{-5}$   $\text{m}/\text{s}$  the highest hydraulic conductivities and the Kusel-layers with  $8.0\cdot10^{-7}$   $\text{m}/\text{s}$  the lowest ones. Hydraulic datasets from wells whose well logs exhibit one or more faults zones show an up to one magnitude higher hydraulic conductivity than

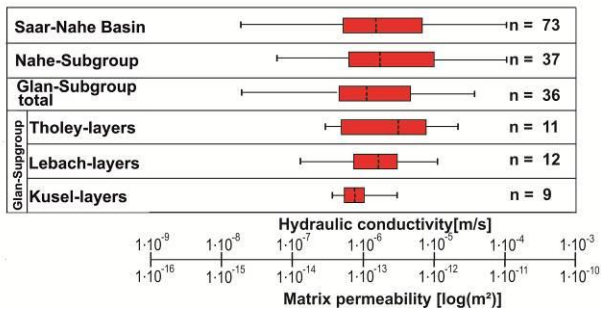


**Figure 8. Box-Whisker-Plot of the hydraulic conductivities ordered according to the main stratigraphic units**

pumping datasets from drillings with no hints on fault zones (Bär, 2012). This phenomenon gives reason to the investigation of the influence of the distance of the nearest fault zone as well as its strike direction on the mean hydraulic conductivity.

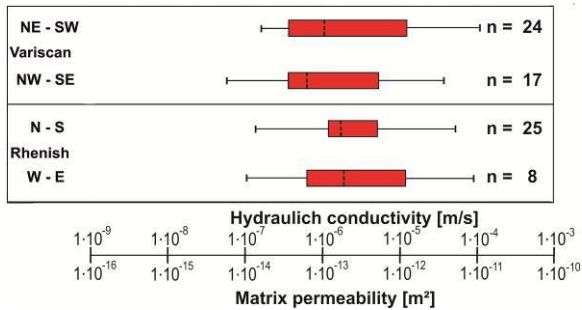


**Figure 9. Box-Whisker-Plot of the hydraulic conductivities ordered according the strike orientation and the superior fault system**

It turned out that the hydraulic conductivities at Rhenish (N-S) striking faults is approximately half a magnitude higher than the hydraulic conductivities at Variscan (SW-NE) striking faults (Fig. 9).

## OUTLOOK

Following the geothermal parameter determination a 3D reservoir model of the northern Upper Rhine Graben will be established based on drilling and seismic data. A depth extrapolation of the hydraulic parameters will be done by the means of the varying depths of the determined test data between 50 and 1,000 m, existing hydraulic test data from reservoir depth coming from the hydrocarbon industry database, knowledge over the orientation and pathways of the mean fault zones as well as the layer thickness distribution in the reservoir. Referring to the procedure of the model by Bär et al. (2011) and Bär (2012) the model shall enable a more accurate prediction of the geothermal reservoir properties in the target horizon. The improved prognosis ability of the reservoir temperatures and production rates connected with this model will allow a clearly improved evaluation of the deep geothermal potential and a better predictability of the exploration risk.

## REFERENCES

Arndt, D., Bär, K., Fritsche, J.-G., Kracht, M., Sass, I. & Hoppe, A.: 3D structural model of the Federal State of Hesse (Germany) for geo-potential evaluation. *Z. dt. Ges. Geowiss.*, 162/4 (2011), 353-370.

Bär, K.: 3D-Modellierung des tiefengeothermischen Potenzials des nördlichen Oberrheingrabens und Untersuchung der geothermischen Eigenschaften des Rotliegend, (2008) 151 S., 64 Abb., 4 Anl., 8 Kt., 1 CD-ROM, unveröff. Diplomarbeit TU Darmstadt.

Bär, K.: Untersuchung der tiefengeothermischen Potenziale von Hessen, (2012) Dissertation, XXVI und 265 S., 111 Abb., 28 Tab., 6 Anh., 1 DVD-ROM, Technische Universität Darmstadt.

Bär, K., Arndt, D., Fritsche, J.-G., Götz, A. E., Kracht, M. Hoppe, A & Sass, I.: 3D-Modellierung der tiefengeothermischen Potenziale von Hessen, – Eingangsdaten und Potenzialausweisung, (2011), *Z. dt. Ges. Geowiss.*, 162/4, 371-388.

Becker, A., Schwarz, M. & Schäfer, A.: Lithostratigraphische Korrelation des Rotliegend im östlichen Saar-Nahe-Becken, (2012) *Jber. Mitt. Oberrhein. geol. Ver.*, 94, 105-133, Stuttgart.

Cooper, H. H., Jacob, C. E.: A generalized graphical method for evaluating formation constants and summarizing well field history, (1946), *Am. Geophys. Union Trans.*, 27, 526-534.

Dickinson, W. R.: Interpreting detrital modes of graywacke and arkose, (1970), *Journal of Sedimentary Petrology*, 40, 695-707.

Gaupp, R., Matter, A., Platt, J., Ramseyer, K. & Walzebuck, J.: Diagenesis and Fluid Evolution of Deeply Buried Permian (Rotliegende) Gas Reservoirs, Northwest Germany, (1993), *The American Association of Petroleum Geologists Bulletin*, 77, No. 7, 1111-1128.

Grötsch, J. & Gaupp, R.: Foreword by the editors. In, Grötsch, J., & Gaupp, R. (eds.): The Permian Rotliegend of the Netherlands, (2011), SEPM Special Publications, 98, 3-6.

Gazzi, P.: Le Arenarie del Flysch Sopracretaceo dell'Appennino Modenese: Correlazioni con il Flysch di Monghidoro, (1966), *Mineralogica e Petrografica Acta* 12, 69-97.

Hornung, J. & Aigner, T.: Sedimentäre Architektur und Poroperme-Analyse fluvialer Sandsteine: Fallbeispiel Coburger Sandstein, Franken, (2004). *Hallesches Jahrb. Geowiss., Reihe B*, 18, 121-138, Halle (Saale).

Klaeske, U.: Untersuchung der hydraulischen Kennwerte des Permokarbons in Hessen und Rheinland-Pfalz, (2012), Dipl.-Arb., TU Darmstadt: 95 S., Darmstadt (unveröff.).

Klinkenberg, L.J.: The permeability of porous media to liquids and gases, (1941), *Drilling Production Practice*, API: 200-213.

Jahn, F., Graham, M. & Cook, M.: Hydrocarbon Exploration & Production, (2008). - Volume 55, Second Edition

(Developments in Petroleum Science), Elsevier Science, 470 S.

Marell, D.: Das Rotliegende zwischen Odenwald und Taunus, (1989). -Geol. Abh. Hessen, 89, 128 S., Wiesbaden.

Müller, H.: Das Permokarbon im nördlichen Oberrheingraben – Paläogeographische und strukturelle Entwicklung des permokarbonen Saar-Nahe-Beckens im nördlichen Oberrheingraben, (1996), *Geol. Abh. Hessen*, 99, 85 S., Wiesbaden.

Lippmann, E. & Rauen, A.: TCS manual / Handbuch zum Thermal Conductivity Scanner, (2005)

Popov, Y.A., Semionov, V.G., Korosteliov, V.M. & Berezin, V.V.: Non-contact evaluation of thermal conductivity of rocks with the aid of a mobile heat source, (1983), *Izvestiya, Physics of the Solid Earth*, 19, 563-567.

Popov, Y.A., Pribnow, D.F.C., Sass, J.H., Williams, C.F., Burkhardt, H.: Complex detailed Investigations of the thermal properties of Rocks on the basis of a moving point Source, (1999), *Earth Physics*, 21, No. 1, *Izvestiya*.

Röhr,C.:[http://www.oberrheingraben.de/Bilder/GK\\_ORG\\_Gross.jpg](http://www.oberrheingraben.de/Bilder/GK_ORG_Gross.jpg), (2006).

Rüther, J.: Thermofazielle Interpretation des Permokarbons im Sprendlinger Horst (2011),, Dipl.-Arb., TU Darmstadt: 105 S., Darmstadt (unveröff.)

Sass, I. & Götz, A.E.: Geothermal reservoir characterization: a thermofacies concept, (2012), *Terra Nova*, 24, 142-147.

Sass, I. & Hoppe, A., Hrsg.: Forschungs- und Entwicklungsprojekt „3D-Modell der geothermischen Tiefenpotenziale von Hessen“ – Abschlussbericht, (2011) ([http://www.energieland-hessen.de/mm/3-D-Modell-HessenEndbericht\\_\(PDF,\\_7.300\\_KB\).pdf](http://www.energieland-hessen.de/mm/3-D-Modell-HessenEndbericht_(PDF,_7.300_KB).pdf))

Schäfer, A.: Variscan molasse in the Saar-Nahe Basin (W-Germany), Upper Carboniferous and Lower Permian, (1989), *Geol. Rdsch.*, 78, 499-524.

Schäfer, A.: Sedimentologisch-numerisch begründeter Stratigraphischer Standard für das Permo-Karbon des Saar-Nahe-Beckens, (2005), *Cour.Forsch.-Inst. Senckenberg*, 254, 369-394, Frankfurt.

Schäfer, A.: Tectonics and sedimentation in the continental strike-slip Saar-Nahe Basin (Carboniferous, West Germany). [Tektonik und Sedimentation im kontinentalen Saar-Nahe-Becken (“Strike-slip”-Modell, Karbon-Perm, Westdeutschland).], (2011), *Z. dt. Ges. Geowiss.*, 162, 127-155, Stuttgart.

Schwarz, M., Becker, A. & Schäfer, A.: Seismische Leithorizonte im nordöstlichen Saar-Nahe-Becken, (2011), *Erdöl Erdgas Kohle*, 127(1), 28-34.

Stollhofen, H.: Vulkaniklastika und Siliziklastika des basalen Oberrotliegend im Saar-Nahe-Becken (SW Deutschland): Terminologie und Ablagerungsprozesse, (1994), *Mainzer geowiss. Mitt.*, 23: 95-138. Mainz.

Stollhofen, H.: Facies architecture variations and seismogenic structures in the Carboniferous-Permian Saar-Nahe Basin (SW Germany): evidence for extension-related transfer fault activity, (1998), *Sedimentary Geology*, 119, 47-83. Elsevier

Theis, C. V.: The relation between the lowering of the piezometric surface and the rate and duration of discharge of a well using groundwater storage, (1935), *Am. Geoph. Union* 16.

Walter, R. & Dorn, P.: Geologie von Mitteleuropa. Schweizerbart, (2007), Stuttgart. X, 511 S.